Journal of Applied Fluid Mechanics, Vol. 9, No. 4, pp. 1615-1625, 2016.
Available online at www.jafmonline.net, ISSN 1735-3572, EISSN 1735-3645.
DOI: 10.18869/acadpub.jafm.68.235.24709

Peristaltic Flow of Phan-Thien-Tanner Fluid in an Asymmetric Channel with Porous Medium

K. Vajravelu[1], S. Sreenadh[2], P. Lakshminarayana[3], G. Sucharitha[3] and M. M. Rashidi[4,5†]

[1]*Department of Mathematics, Department of Mechanical, Materials and Aerospace Engineering, University of Central Florida, Orlando, Florida 32816 - 1364, USA*
[2]*Department of Mathematics, Sri Venkateswara University, Tirupati 517 502, India*
[3]*Department of Mathematics, Sree Vidyanikethan Engineering College, Tirupati 517 102, India*
[4]*Shanghai Key Lab of Vehicle Aerodynamics and Vehicle Thermal Management Systems, Address: 4800 Cao, China*
[5]*ENN-Tongji Clean Energy Institute of advanced studies, Shanghai, China*

†*Corresponding Author Email: mm_rashidi@tongji.edu.cn*

(Received February 17, 2015; accepted August 23, 2015)

ABSTRACT

This paper deals with peristaltic transport of Phan-Thien-Tanner fluid in an asymmetric channel induced by sinusoidal peristaltic waves traveling down the flexible walls of the channel. The flow is investigated in a wave frame of reference moving with the velocity of the waveby using the long wavelength and low Reynolds number approximations.The nonlinear governing equations are solved employing a perturbation method by choosing We as the perturbation parameter. The expressions for velocity, stream function and pressure gradient are obtained. The features of the flow characteristics are analyzed through graphs and the obtained results are discussed in detail. It is noticed that the peristaltic pumping gets reduced due to an increase in the phase difference of the traveling waves. It is also observed that the size of the trapping bolus is a decreasing function of the permeability parameter σ and the Weissenberg number. Furthermore, the results obtained for the flow characteristics reveal many interesting behaviors that warrant further study on the non-Newtonian fluid phenomena, especially the Peristaltic flow phenomena.

Keywords: Trapping phenomena; Peristaltic transport; Phan-thien-tanner fluid; Porous medium; Asymmetric channel.

NOMENCLATURE

$a_1,\ b_1$	amplitudes of the waves
c	wave speed
d_1+d_2	width of the channel
d/dt	material derivative
k	relaxation time
k_0	permeability
p	pressure
Re	Reynolds numbers respectively
$\boldsymbol{s}^{\nabla}$	Oldroyd's upper-convected derivative
t	time
tr	trace
$(\overline{u},\overline{v})$	velocities in wave frame
We	Weissenberg number
$(\overline{X},\overline{Y})$	where $\overline{X}-$ and $\overline{Y}-$ axes are taken respectively parallel and transverse to the direction of wave propagation
μ	dynamic viscosity
ϕ	phase difference varying in the range $0\le\phi\le\pi$.
λ	wave length
$(\overline{U},\overline{V})$	velocities in laboratory frame
$\overline{P},\overline{p}$	pressures in the laboratory and wave frames respectively.
δ	wavenumber
σ	permeability parameter.

1. INTRODUCTION

Peristalsis is a mechanism for pumping fluid in a tube by means of a moving contractile ring around the tube, which pushes the material onward. The peristaltic wave generated along the flexible wall

of the tube provides an efficient means for the transport of fluids in living organisms and in industrial pumping. It is an inherent property of many smooth muscle tubes, since stimulation at any point causes a contractile ring around the tube. In general, peristalsis induces two types of fluid movements, namely propulsive and mixing. The peristaltic propulsive movement is observed in the esophagus, bileduct, the ureter and other glandular ducts through the body. The mixing property of peristalsis is speculated to be in the digestion of food in stomach and such other biological systems. Also the principle of peristalsis is adapted by engineers to pump the industrial fluids which are to be kept away from the pumping machinery. Shapiro *et al*. (1969) reported initial studies on peristaltic flow of viscous fluid. Since then, the mathematical models obtained by a train of periodic sinusoidal waves in an infinitely long two-dimensional symmetric channel or axisymmetric tubes containing Newtonian or non-Newtonian fluid were investigated by several researchers (Jaffrin and Shapiro, 1971; Shukla and Gupta, 1982; Srivastava and Srivastava, 1984; Mishra and Ramachandra Rao, 2003;Vajravelu *et al*., 2005a, 2005b).

In recent years, physiologists observed that the intra-uterine fluid flow due to myometrial contractions is peristaltic type of motion and it may occur in both symmetric and asymmetric channels (Devries *et al*., 1990). Eytan *et al*. (1999) reported that the non-pregnant woman uterine contractions are very complicated since they are composed of variable amplitudes, a range of frequencies, and different wave lengths. Also, observed that the width of the sagittal cross-section of the uterine cavity increases toward the fundus and the cavity is not fully occluded during the contractions. Eytan and Elad (1999) developed a mathematical model of peristaltic flow induced by wave trains with phase differences moving independently on the upper and lower walls to simulate intra uterine fluid motion in the sagittal cross section of the uterus. They have obtained a time dependent flow solution in a fixed frame through the lubrication approach.

As we know, there are certain biofluids (for example, blood, saliva, gastric juice) whose characteristics cannot be described by the Newton's law of velocity, especially those with high molecular weight leads to the development of non-Newtonian fluid mechanics. Hence some investigators have recently engaged in making progress in peristaltic flows of non-Newtonian fluids (Elshehawey and Mekhemier, 1994; Usha and Ramachandra Rao,1997; Kothandapani and Srinivas, 2008; Hakeem and Naby, 2009; Nadeem and Akram, 2010;Narahari and Sreenadh, 2010; Sreenadh *et al*., 2011; Hayat *et al*., 2011, 2012a, 2012b;Noreen Sher Akbar and Nadeem, 2012; Vajravelu *et al*., 2009, 2012, 2014; Sucharitha *et al*., 2013; Rathod and Laxmi, 2014; Riaz *et al*., 2014; Noreen and Nadeem 2014;Hina *et al*., 2015; Ravikiran, and Radhakrishnamacharya, 2015).
For solving non-linear differential equations, we employ pure numerical approach and/or analytical approach. Both of these approaches have their own advantages and disadvantages. Scientists and engineers follow one or both the approaches to resolve and study their mathematical models for better understanding and application. Analytical methods contain: Perturbation method (PM), Adomian decomposition method (ADM), homotopy analysis method (HAM), optimal homotopy asymptotic Method (OHAM), differential transform method (DTM) etc. (for details see Beg *et al*. 2013, 2014; Rashidi *et al*. 2009; and Edalatpanah and Rashidi 2014). These methods have certain advantages over the commonly used numerical methods.

Viscous flow through a porous medium is of fundamental importance in ceramic engineering, ground water hydrology, petroleum technology, powder metallurgy, industrial filtration and such other fields. Also, in the springs of the geothermal region, water is known to be an electrically conducting fluid. Flow through porous media has been studied by a number of researchers (Srinivas and Kothandapani, 2009; Lakshminarayana *et al*., 2013; Anjali Devi and Kayalvizhi, 2010, 2013; Tripathi, 2013; Agoor andEldabe, 2014; Ramesh and Devakar, 2015). Hayat *et al*. (2008) investigated the influence of partial slip on the peristaltic flow in a porous medium. The Effect of heat transfer on the peristaltic flow of an electrically conducting fluid in a porous space was studied by Hayat *et al*. (2009). Vajravelu *et al*. (2011) discussed the influence of heat transfer on the peristaltic transport of a Jeffrey fluid in a vertical porous stratum. Singh and Rathee (2011) presented the analysis of non-Newtonian blood flow through stenosed vessel in a porous medium under the effect of magnetic field.

Motivated by the above studies, in the present paper, the peristaltic transport of Phan-Thien-Tanner fluid in an asymmetric channel with porous medium is investigated. The governing equations of Phan-Thien-Tanner fluid model are solved by a perturbation technique. The expressions for stream function, pressure gradient and pressure rise have been obtained. The effects of various physical parameters on the velocity, the pressure rise and the trapping phenomenon are discussed through graphs.

2. MATHEMATICALFORMULATION

We consider an incompressible Phan-Thien-Tanner fluid flow in an asymmetric channel with porous medium, of width $d_1 + d_2$. Let c be the speed by which sinusoidal wave trains propagate along the channel walls. Consider the rectangular coordinate system $\left(\overline{X}, \overline{Y}\right)$ where $\overline{X}$ and $\overline{Y}$ − axes are taken respectively parallel and transverse to the direction of wave propagation. The wall surfaces are modeled by

$$\bar{Y} = H_1 = d_1 + a_1 Cos\left[\frac{2\pi}{\lambda}\left(\bar{X} - c\bar{t}\right)\right],$$

$$\bar{Y} = H_2 = -d_2 - b_1 Cos\left[\frac{2\pi}{\lambda}\left(\bar{X} - c\bar{t}\right) + \phi\right], \tag{2.1}$$

where ϕ is the phase difference varying in the range $0 \le \phi \le \pi$. Here, $\phi = 0$ correspond to symmetric channel with waves out of phase and $\phi = \pi$ with waves in phase, and further a_1, b_1, d_1, d_2 *and* ϕ satisfy the condition $a_1^2 + b_1^2 + 2a_1 b_1 \cos\phi \le (d_1 + d_2)^2$ so that walls will not intersect with each other. The basic equations of motion are the following:

Continuity equation

$$\nabla . \boldsymbol{V} = 0. \tag{2.2}$$

Momentum equation

$$\rho \frac{d\boldsymbol{V}}{dt} = div\boldsymbol{T}. \tag{2.3}$$

The constitutive equations for PTT model are

$$\boldsymbol{T} = -p\boldsymbol{I} + \boldsymbol{s}, \tag{2.4}$$

$$f\left(tr(\boldsymbol{s})\right)\boldsymbol{s} + k\boldsymbol{s}^{\nabla} = 2\mu\boldsymbol{D}, \tag{2.5}$$

$$s^{\nabla} = \frac{ds}{dt} - s.L^* - L.s, \tag{2.6}$$

$$\boldsymbol{L} = grad\boldsymbol{V}, \tag{2.7}$$

where p is the pressure, I is the identity tensor, Vis the velocity, T is the Cauchy stress tensor, μ is the dynamic viscosity, sis an extra-stress tensor, D is the deformation-rate tensor, k is the relaxation time, $\boldsymbol{s}^{\nabla}$ denotes Oldroyd's upper-convected derivative, d/dt the material derivative, tr is the trace and asterisk denotes the transpose.

Function f in the linearized PTT model which satisfies

$$f\left(tr\left(\boldsymbol{s}\right)\right) = 1 + \frac{\varepsilon k}{\mu} tr(\boldsymbol{s}). \tag{2.8}$$

Note that the PTT model reduces to an upper convected Maxwell model (UCM) when the extensional parameter $\varepsilon$is zero.

We introduce the transformations between fixed and wave frames as

$$\begin{aligned} &\bar{x} = \bar{X} - c\bar{t}, \ \bar{y} = \bar{Y}, \ \bar{u} = \bar{U} - c, \\ &\bar{v} = \bar{V}, \ \bar{p}\left(\bar{x}\right) = \bar{P}\left(\bar{X}, \bar{t}\right), \end{aligned} \tag{2.9}$$

Using the equation (2.9) the governing equations in the wave frame can be written as

$$\frac{\partial \bar{u}}{\partial \bar{x}} + \frac{\partial \bar{v}}{\partial \bar{y}} = 0, \tag{2.10}$$

$$\rho\left[\bar{u}\frac{\partial}{\partial \bar{x}} + \bar{v}\frac{\partial}{\partial \bar{y}}\right]\bar{u} = -\frac{\partial \bar{p}}{\partial \bar{x}} + \frac{\partial \bar{S}_{\bar{x}\bar{x}}}{\partial \bar{x}} + \frac{\partial \bar{S}_{\bar{x}\bar{y}}}{\partial \bar{y}} - \frac{\mu}{k_0}(\bar{u} + c), \tag{2.11}$$

$$\rho\left[\bar{u}\frac{\partial}{\partial \bar{x}} + \bar{v}\frac{\partial}{\partial \bar{y}}\right]\bar{v} = -\frac{\partial \bar{p}}{\partial \bar{y}} + \frac{\partial \bar{S}_{\bar{y}\bar{x}}}{\partial \bar{x}} + \frac{\partial \bar{S}_{\bar{y}\bar{y}}}{\partial \bar{y}} - \frac{\mu}{k_0}\bar{v}, \tag{2.12}$$

$$f\bar{S}_{\bar{x}\bar{x}} + k\left[\bar{u}\frac{\partial \bar{S}_{\bar{x}\bar{x}}}{\partial \bar{x}} + \bar{v}\frac{\partial \bar{S}_{\bar{x}\bar{x}}}{\partial \bar{y}} - 2\frac{\partial \bar{u}}{\partial \bar{x}}\bar{S}_{\bar{x}\bar{x}} - 2\frac{\partial \bar{u}}{\partial \bar{y}}\bar{S}_{\bar{x}\bar{y}}\right]\bar{v} = 2\mu\frac{\partial \bar{u}}{\partial \bar{x}}, \tag{2.13}$$

$$f\bar{S}_{\bar{x}\bar{x}} + k\left[\bar{u}\frac{\partial \bar{S}_{\bar{y}\bar{y}}}{\partial \bar{x}} + \bar{v}\frac{\partial \bar{S}_{\bar{y}\bar{y}}}{\partial \bar{y}} - 2\frac{\partial \bar{v}}{\partial \bar{x}}\bar{S}_{\bar{y}\bar{x}} - 2\frac{\partial \bar{v}}{\partial \bar{y}}\bar{S}_{\bar{y}\bar{y}}\right]\bar{v} = 2\mu\frac{\partial \bar{v}}{\partial \bar{y}}, \tag{2.14}$$

$$f\bar{S}_{\bar{z}\bar{z}} + k\left[\bar{u}\frac{\partial \bar{S}_{\bar{z}\bar{z}}}{\partial \bar{x}} + \bar{v}\frac{\partial \bar{S}_{\bar{z}\bar{z}}}{\partial \bar{y}}\right] = 0, \tag{2.15}$$

$$f\bar{S}_{\bar{x}\bar{y}} + k\left[\bar{u}\frac{\partial \bar{S}_{\bar{x}\bar{y}}}{\partial \bar{x}} + \bar{v}\frac{\partial \bar{S}_{\bar{x}\bar{y}}}{\partial \bar{y}} - \frac{\partial \bar{v}}{\partial \bar{x}}\bar{S}_{\bar{x}\bar{x}} - \frac{\partial \bar{v}}{\partial \bar{y}}\bar{S}_{\bar{x}\bar{y}} - \frac{\partial \bar{u}}{\partial \bar{x}}\bar{S}_{\bar{x}\bar{y}} - \frac{\partial \bar{u}}{\partial \bar{y}}\bar{S}_{\bar{y}\bar{y}}\right] = \mu\left(\frac{\partial \bar{u}}{\partial \bar{y}} + \frac{\partial \bar{v}}{\partial \bar{x}}\right), \tag{2.16}$$

$$f = 1 + \frac{\varepsilon k}{\mu}(\bar{S}_{\bar{x}\bar{x}} + \bar{S}_{\bar{y}\bar{y}} + \bar{S}_{\bar{z}\bar{z}}). \tag{2.17}$$

The boundary conditions are

$$\begin{aligned} &\bar{\psi} = \frac{q}{2}, \ \bar{u} = \frac{\partial \bar{\psi}}{\partial \bar{y}} = -c \quad at \ \bar{y} = H_1 \\ &\bar{\psi} = -\frac{q}{2}, \ \bar{u} = \frac{\partial \bar{\psi}}{\partial \bar{y}} = -c \ at \ \bar{y} = H_2. \end{aligned} \tag{2.17a}$$

The non-dimensional quantities and the expressions for velocity in terms of stream function are given by

$$\left.\begin{aligned} &x = \frac{\bar{x}}{\lambda}, y = \frac{\bar{y}}{d_1}, u = \frac{\bar{u}}{c}, v = \frac{\bar{v}}{\delta c}, \delta = \frac{d_1}{\lambda}, p = \frac{d_1^2 \bar{p}}{\mu c \lambda}, t = \frac{c\bar{t}}{\lambda}, \\ &h_1 = \frac{H_1}{d_1}, h_2 = \frac{H_2}{d_1}, \mathrm{Re} = \frac{\rho c d_1}{\mu}, d = \frac{d_2}{d_1}, a = \frac{a_1}{d_1}, b = \frac{b_1}{d_1}, \\ &S_{ij} = \frac{\bar{S}_{ij} d_1}{\mu c}, We = \frac{kc}{d_1}, \sigma = \frac{d_1}{\sqrt{k_0}}, F = \frac{q}{c d_1}, \psi = \frac{\bar{\psi}}{c d_1}, \\ &\text{and} \ u = \frac{\partial \psi}{\partial y}, v = -\frac{\partial \psi}{\partial x}. \end{aligned}\right\} \tag{2.18}$$

The conditions in (2.1) can be written as

$$h_1 = 1 + a\cos(2\pi x),\ h_2 = -d - b\cos(2\pi x + \phi). \tag{2.19}$$

Using the above non-dimensional quantities and the long wavelength approximation the basic equations reduce to

$$\frac{dp}{dx} = \frac{\partial S_{xy}}{\partial y} - \sigma^2\left(\frac{\partial \psi}{\partial y} + 1\right), \tag{2.20}$$

$$\frac{\partial p}{\partial y} = 0, \tag{2.21}$$

$$f\ S_{xx} = 2We\frac{\partial^2 \psi}{\partial y^2} S_{xy}, \tag{2.22}$$

$$f\ S_{yy} = 0, fS_{zz} = 0, \tag{2.23}$$

$$f\ S_{xx} = -We\frac{\partial^2 \psi}{\partial y^2} S_{yy} + \frac{\partial^2 \psi}{\partial y^2}, \tag{2.24}$$

and the non-dimensional boundary conditions are

$$\psi = \frac{F}{2},\ \frac{\partial \psi}{\partial y} = -1 \ \ at\ \ y = h_1 = 1 + a\cos(2\pi x),$$
$$\psi = -\frac{F}{2},\ \frac{\partial \psi}{\partial y} = -1\ at\ \ y = h_2 = -d - b\cos(2\pi x + \phi), \tag{2.25}$$

where F is the mean flow rate in the wave frame.

The flux at any axial station in the fixed frame is

$$Q = \int_{h_2}^{h_1} (u+1)dy = h_1 - h_2 + F. \tag{2.26}$$

The average volume flow rate over one period of the peristaltic wave is defined as

$$\Theta = \frac{1}{T}\int_0^T Q dt = \frac{1}{T}\int_0^T (h_1 - h_2 + F)dt = F + 1 + d. \tag{2.27}$$

From the equation (2.23) we have $S_{yy} = 0, S_{zz} = 0$ and from equation (2.20) we get

$$S_{xy} = y\frac{dp}{dx} + \sigma^2(\psi + y). \tag{2.28}$$

With the help of (2.23) and (2.24) we can write

$$S_{xx} = 2We\, S_{xy}^2. \tag{2.29}$$

From the equations (2.17), (2.23) and (2.29) we obtain

$$\frac{\partial^2 \psi}{\partial y^2} = S_{xy} + 2\varepsilon We^2 S_{xy}^3. \tag{2.30}$$

Substituting (2.28) into (2.30) we get

$$\frac{\partial^2 \psi}{\partial y^2} = y\frac{dp}{dx} + \sigma^2(\psi + y) + 2\varepsilon We^2\left(y\frac{dp}{dx} + \sigma^2(\psi + y)\right)^3. \tag{2.31}$$

3. PERTURBATION SOLUTION

Equation (2.31) is non-linear, its exact solution is not possible, and hence we employ the perturbation technique to find the solution. For perturbation solution, we expand the flow quantities in a power series of the small parameter We^2 as follows:

$$\left.\begin{aligned} \psi &= \psi_0 + We^2\psi_1 + O(We^4) \\ F &= F_0 + We^2 F_1 + O(We^4) \\ \phi &= \phi_0 + We^2\phi_1 + O(We^4) \\ \frac{dp}{dx} &= \frac{dp_0}{dx} + We^2\frac{dp_1}{dx} + O(We^4) \end{aligned}\right\}. \tag{3.1}$$

Using the above expressions in equations (2.25) and (2.31), we obtain a system of equations of different orders.

3.1 System of Order We^0

The governing equations and boundary conditions of the zeroth-order problem are

$$\frac{\partial^2 \psi_0}{\partial y^2} = y\frac{dp_0}{dx} + \sigma^2(\psi_0 + y), \tag{3.2}$$

$$\psi_0 = \frac{F_0}{2}, \frac{\partial \psi_0}{\partial y} = -1 \ \ at\ \ y = h_1 = 1 + a\cos(2\pi x),$$
$$\psi_0 = -\frac{F_0}{2}, \frac{\partial \psi_0}{\partial y} = -1\ at\ \ y = h_2 = -d - b\cos(2\pi x + \phi). \tag{3.3}$$

The solution of the zeroth - order problem is given by

$$\psi_0 = c_1\cosh\sigma y + c_2\sinh\sigma y - y\left(\frac{1}{\sigma^2}\frac{dp_0}{dx} + 1\right), \tag{3.4}$$

and the axial velocity is

$$u_0 = \sigma c_1\sinh\sigma y + \sigma c_2\cosh\sigma y - \left(\frac{1}{\sigma^2}\frac{dp_0}{dx} + 1\right). \tag{3.5}$$

3.2 System of Order We^2

The governing equations and boundary conditions of the first-order problem are

$$\frac{\partial^2 \psi_1}{\partial y^2} = y\frac{dp_1}{dx} + \sigma^2\psi_1 + 2\varepsilon\left(y\frac{dp_0}{dx} + \sigma^2(\psi_0 + y)\right)^3, \tag{3.6}$$

$$\psi_1 = \frac{F_1}{2}, \frac{\partial \psi_1}{\partial y} = 0 \quad at \quad y = h_1,$$
$$\psi_1 = -\frac{F_1}{2}, \frac{\partial \psi_1}{\partial y} = 0 \quad at \quad y = h_2. \tag{3.7}$$

The solution of the first-order problem is given by

$$\begin{aligned}\psi_1 =& c_3 \cosh\sigma y + c_4 \sinh\sigma y - y\left(\frac{1}{\sigma^2}\frac{dp_0}{dx} + 1\right) \\ &+ L_{31} y^3 - L_{15} y^2 + L_{32} y \\ &+ \frac{1}{4}\left(L_5 \cosh 3\sigma y + L_6 \sinh 3\sigma y\right) + \cosh 2\sigma y \left(L_{34} + L_{33} y\right) \\ &+ \sinh 2\sigma y \left(L_{36} + L_{35} y\right) \\ &+ \sinh\sigma y \begin{pmatrix} L_{27} + L_{37} y - L_{38} y^2 \\ + L_{39} y^3 - L_{40} y^4 + L_{41} y^5 - L_{42} y^6 \end{pmatrix} \\ &+ \cosh\sigma y \begin{pmatrix} L_{28} + L_{43} y - L_{44} y^2 \\ + L_{45} y^3 - L_{46} y^4 + L_{47} y^5 - L_{48} y^6 \end{pmatrix},\end{aligned} \tag{3.8}$$

and the corresponding first-order axial velocity is

$$\begin{aligned}u_1 =& \sigma c_3 \sinh\sigma y + \sigma c_4 \cosh\sigma y - \frac{1}{\sigma^2}\frac{dp_1}{dx} + 3L_{31} y^2 - 2L_{15} y \\ &+ L_{32} + \frac{3\sigma}{4}\left(L_5 \sinh 3\sigma y + L_6 \cosh 3\sigma y\right) \\ &+ \sinh 2\sigma y \left(L_{71} + 2\sigma L_{33} y\right) + \cosh 2\sigma y \left(L_{72} + 2\sigma L_{35} y\right) \\ &+ \sinh\sigma y \left(L_{73} + L_{74} y + L_{75} y^2 + L_{76} y^3 + L_{77} y^4 + L_{78} y^5\right) \\ &+ \cosh\sigma y \left(L_{79} + L_{80} y + L_{81} y^2 + L_{82} y^3 + L_{83} y^4 + L_{84} y^5\right).\end{aligned} \tag{3.9}$$

The final expression for the axial velocity is given by

$$u = u_0 + We^2 u_1. \tag{3.10}$$

The pressure gradient is obtained as

$$\frac{dp}{dx} = \frac{dp_0}{dx} + We^2 \frac{dp_1}{dx} \tag{3.11}$$

where

$$\frac{dp_0}{dx} = \sigma^2\left(\frac{F_0}{L_4^1} - 1\right) \text{ and } \quad \frac{dp_1}{dx} = \frac{F_1 - L_{132}}{L_{131}}. \tag{3.12}$$

The non-dimensional pressure rise and the non-dimensional friction forces per unit wave length in the wave frame are given by

$$\Delta p = \int_0^1 \frac{dp}{dx} dx, \tag{3.13}$$

$$F_1 = \int_0^1 (-h_1)\frac{dp}{dx} dx, \tag{3.14}$$

$$F_2 = \int_0^1 (-h_2)\frac{dp}{dx} dx. \tag{3.15}$$

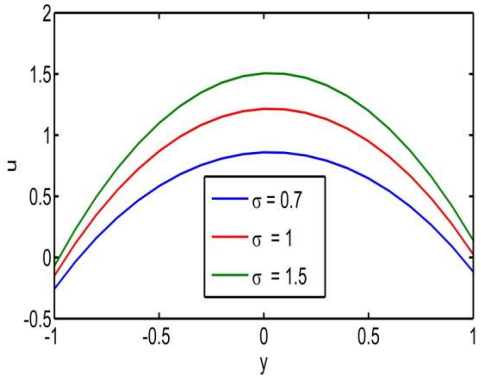

Fig. 1. Velocity profiles for different σ with fixed a=0.4, b=0.4, d=1, ø=π/8, F=1.5, We=0.01.

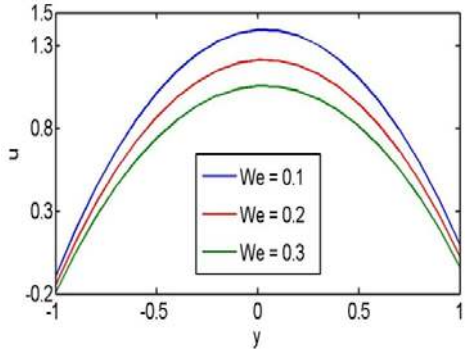

Fig. 2. Velocity profiles for different We with fixed a=0.4, b=0.4, d=1, ø=π/8, F=1.5, σ=1.5.

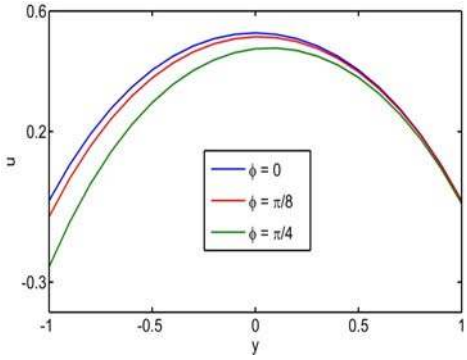

Fig. 3. Velocity profiles for different ϕ with fixed a=0.4, b=0.4, d=1, F=1.5, σ=1.5, We=0.05.

4. RESULTS AND DISCUSSION

The expression for velocity in terms of y is given by the equation (3.10). Velocity profiles are plotted in Figures 1-6 to study the effects of the different parameters such as the permeability parameter σ,

Weissenberg number We, phase difference ϕ and amplitudes a, b on the velocity distribution. Fig.1 and Fig.2 are drawn to study the effect of σ and We. We notice that the velocity profiles are parabolic. Also observe that the velocity increases with decreasing and We increasing σ. This may be due to the increment of elastic forces over the viscous forces in the non-Newtonian fluid flow. Further the increase in the permeability reduces resistive forces and hence increases the fluid velocity in the channel. From Fig.3, we notice that the velocity decreases with an increase in ϕ. Fig.4 and Fig.5 are plotted to study the effects of a and b on the velocity. We observe that the velocity increases with increasing a,b. Fig.6 depicts that the velocity decreases with an increase in d.

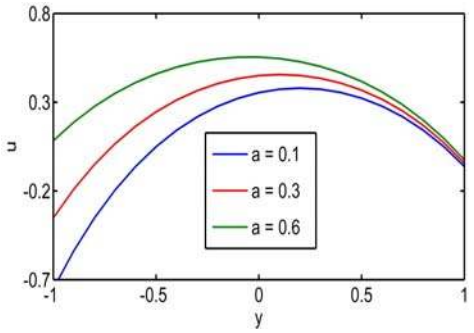

Fig. 4. Velocity profiles for different a with fixed b=0.4, d=1, x=0, ø=π/8, F=1.5, σ=1.5, We=0.15.

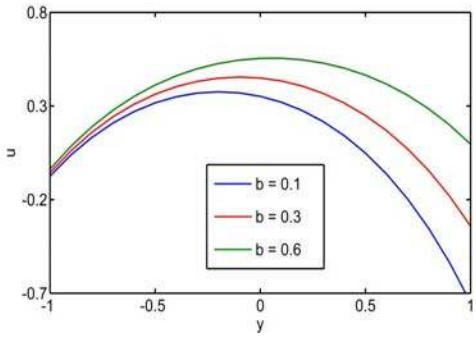

Fig. 5. Velocity profiles for different b with fixed a=0.4, x=0, d=1, ø=π/8, F=1.5, σ=1.5, We=0.15.

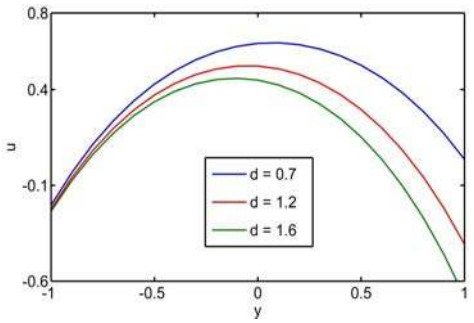

Fig. 6. Velocity profiles for different d with fixed a=0.4, b=0.4, x=0, ø=π/8, F=1.5, σ=1.5, We=0.15.

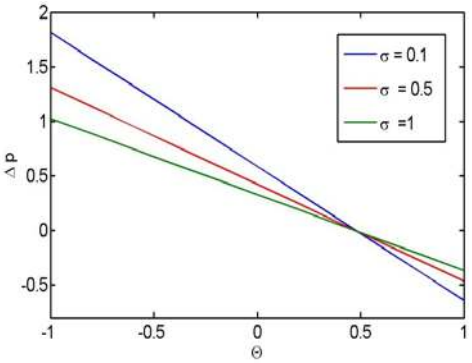

Fig. 7. Velocity profiles for different σ with fixed a=0.4, b=0.4, d=1, ø=π/8, We=0.15.

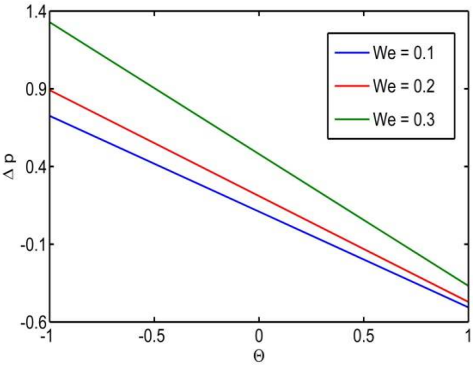

Fig. 8. Velocity of pressure rise for different We with fixed a=0.4, b=0.4, d=1, ø=π/8, σ=1.5.

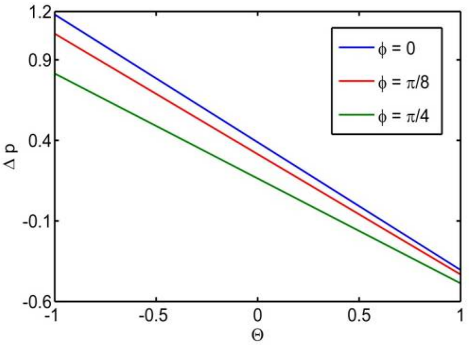

Fig. 9. Velocity of pressure rise for different ϕ with fixed a=0.4, b=0.4, d=1, We=0.02, σ=1.5.

We have calculated the pressure rise Δp in terms of the mean flow rate Θ from equation (3.11). Fig.7 shows the effect of σ on Δp. We observe that for a given Θ, the pressure rise decreases with increasing σ initially and coincide at a point $(0.5,0)$ and after this point the situation is reversed. The effect of We is shown in Fig.8. It can be seen that the pressure rise increases with an increase in We which is due to the enhancement of frictional forces in the channel. From Fig.9 we observe that the pressure rise decreases with

increasing ϕ. From Fig.10, we notice that the frictional forces have the opposite behavior when compared with the pressure rise.

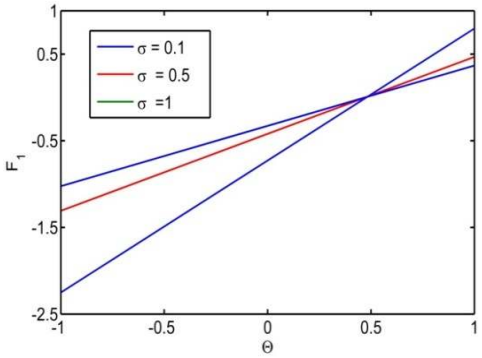

Fig. 10. Variation of frictional force (at y=h1) for different σ with fixed a=0.4, b=0.4, d=1, ø=π/8 We=0.02.

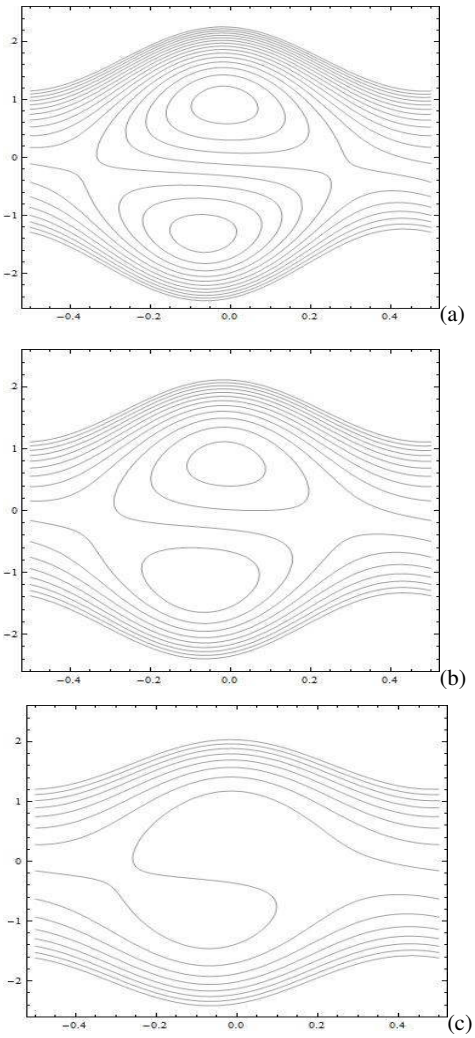

Fig. 11. Streamlines for a=0.3, b=1.3, ø=π/6, We=0.001, F=10 and for different values of σ(a) σ=1, (b)σ1.05, (c)σ=1.15.

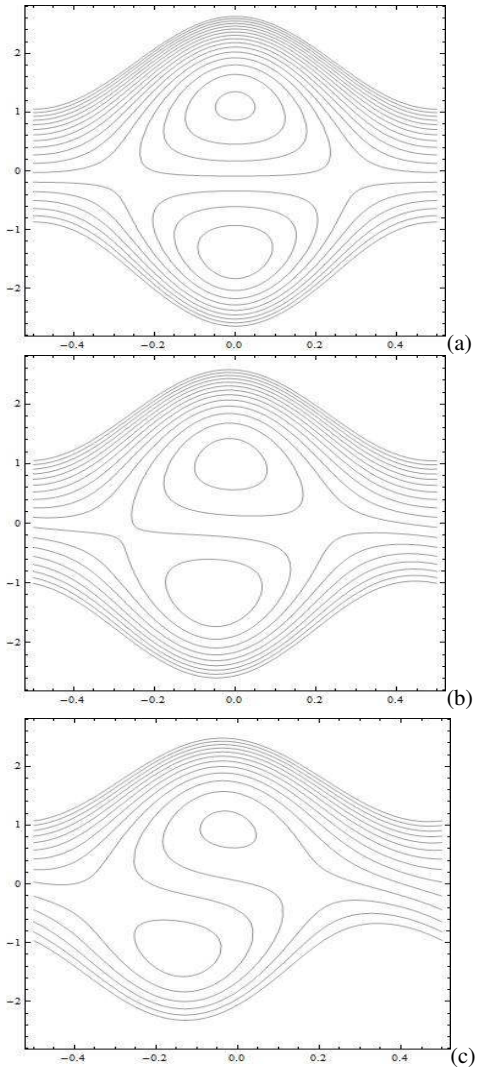

Fig. 12. Streamlines for a=0.3, b=0.3, d=1.2, σ=1, We=0.001, F=10 and for different values of ø(a) ø=0, (b)ø=π/8, (c) ø =π/3.

The results obtained for pumping characteristics are validated with the work of Hayat *et al*. (2011). They reported that Δp has direct relation to Hartmann number and the applied magnetic field provides hindrance to flow. In the present analysis porous medium resists the flow similar to applied magnetic field. Our results agree well with the behavior of the pressure rise due to the influence of permeability $k\ (\text{or}\,\sigma^{-1})$ which is similar to the results of Hayat *et al*. (2011) for Hartmann number. Further it is noticed that the present work (for porous medium) and the results of Hayath *et al*. (2011) (for magnetic case) yield similar conclusions on the effect of phase difference ϕ of the peristaltic waves describing the asymmetry of the channel.

5. TRAPPINGPHENOMENA

The formation of an internally circulating bolus of

fluid by closed streamlines is called trapping and this trapped bolus is pushed ahead with the peristaltic wave. The effects of σ, ϕ and *We* on the streamlines are shown in Figures 11 to 13. It is observed that the size of the trapping bolus decreases with increasing σ, ϕ and *We* Also it is noticed that the bolus disappears at $\sigma = 1.15$ and $We = 0.02$.

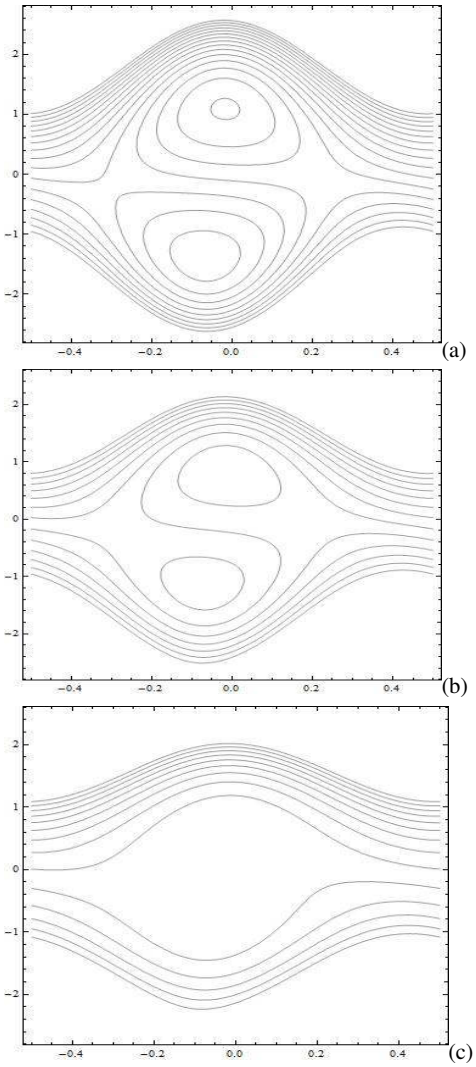

Fig. 13. Streamlines for a=0.3, b=0.3, d=1.3, σ=1, ø=π/6, F=10 and for different values of We (a) We =0.001, (b) We =0.01, (c) We =0.02.

6. CONCLUSIONS

The peristaltic transport of Phan-Thien-Tanner fluid in an asymmetric channel with porous medium under the assumptions of long wavelength and low Reynolds number is studied in this paper. The analytical expressions are obtained for the velocity, stream function and pressure gradient. The features of the flow characteristics are analyzed by plotting graphs and discussed in detail.

- We observe that the velocity increases with increasing permeability parameter σ and amplitudes a, b. The velocity decreases with an increase in Weissenberg number We, phase difference ϕ and amplitude *d*.
- The pressure rise decreases with increasing σ in the pumping region and opposite behavior is observed in the co-pumping region. Also the pressure rise increases with an increase in We whereas it decreases with increasing ϕ .
- We notice that both the frictional forces have the opposite behavior when compared with the pressure rise.
- It is observed that the size of the trapping bolus decreases with increasing σ, ϕ and We .
- The results obtained for pumping and co-pumping regions are validated with the work of Hayat *et al*. (2011).

ACKNOWLEDGEMENT

We thank the reviewers for the constructive and helpful comments that lead to definite improvement in the paper.

REFERENCES

Agoor, B. M. and N. T. M. Eldabe (2014).Rayleigh-Taylor instability at the interface of superposed Couple-stress Casson fluids flow in porous medium under the effect of a magnetic field. *Journal of Applied Fluid Mechanics* 7(4), 573-580.

Anjali Devi, S. P. and M. Kayalvizhi (2013). Nonlinear hydromagnetic flow with radiation and heatsource over a stretching surface with prescribed heat and mass flux embedded in a porous medium.*Journal of Applied Fluid Mechanics* 6(2), 157-165.

Anjali Devi, S. P. and M. Kayalvizhi (2010).Viscous dissipation and radiation effects on thethermal boundary layer flow with heat and mass transfer over a non-isothermal stretchingsheet with internal heat generation embedded in a porous medium.*International Journal of Engineering and Technology* 2(20), 1-10.

Anwar Bég, O., M. Keimanesh, M. M. Rashidi and M. Davoodi (2013). Multi-Step DTM Simulation of Magneto-Peristaltic Flow of a Conducting Williamson Viscoelastic Fluid.*International Journal of Applied Mathematics and Mechanics* 9(12), 22-40.

Anwar Bég, O., U. S. Mahabaleswar, M. M. Rashidi, N. Rahimzadeh, J. L. Curiel Sosa, I. Sarris and N. Laraqi (2014). Homotopy Analysis of Magneto-hydrodynamic Convection Flow in Manufacture of a Viscoelastic Fabric for Space Applications. *International Journal of Applied Mathematics and Mechanics* 10(10), 9-49.

Arshad Riaz, S., N. R. Ellahi and Noreen Sher Akbar (2014). Series solution of unsteady peristaltic flow of a Carreau fluid in small intestines. .*Int. J. of Biomath.* 7(5), 14500491.

Devries, K., E. A. Lyons, G. Ballard, C. S. Levi and D. J. Lindsay (1990). Contractions of the inner third of the myometriu. *Am. J. Obstet. Gynecol.*162, 679–682.

Edalatpanah, S. A. and M. M. Rashidi (2014). On the Application of Homotopy Perturbation Method for Solving Systems of Linear Equations. *International Scholarly Research Notices.*Article ID 143512, 5.

Elshehawey, E. F. and Kh. S. Mekhemier (1994). Couple-Stresses in peristaltic transport of fluids. *J. Phys. D: Appl. Phys.* 27, 1163.

Eytan, O. and D. Elad (1999). Analysis of intrauterine motion induced by uterine contractions *Bull. Math. Biol.* 61, 221–238.

Eytan, O., A. J. Jaffa, J. Har-Toov, E. Dalach and D. Elad (1999). Dynamics of the intrauterine fluid wall interface. *Ann. Biomed. Eng.* 27, 372–379.

Hakeem, A. E. and A. E. Naby (2009). Creeping flow of Phan-Thien–Tanner fluids in a peristaltic tube with an infinite long wavelength. *J. Appl. Mech.* 76(6), 064504.

Hayat, T., M. U. Quereshi and Q. Hussain (2009). Effect of heat transfer on the peristaltic flow of an electrically conducting fluid in a porous space.

Hayat, T., Q. Hussain and N. Ali (2008). Influence of partial slip on the peristaltic flow in a porous medium. *Physica A.* 387**,** 3399–3409.

Hayat, T., S. Noreen and A. Hendi (2011). Peristaltic motion of Phan-Thien-Tanner fluid in the presence of slip condition.*Journal of Biorheology* 25(1), 8-17.

Hayat, T., S. Noreen, N. Ali and S. Abbasbanday (2012). Peristaltic motion of Phan-Thien-Tanner fluid ina planar channel. *Numerical Methods for Partial Differential Equations* 28(3), 737–748.

Hayat, T., S. Noreen, S. Asghar and Awatifa Hendi (2011). Influence of an induced magnetic field on peristaltic transport of a Phan-Thien-Tanner fluid in an asymmetric channel.*Chemical Engineering Communications* 198(5), 609–628.

Hina, S., M. Mustafa, T. Hayat and N. D. Alotaibi (2015). On peristaltic motion of pseudoplastic fluid in a curved channel with heat/mass transfer and wall properties. *Applied Mathematics and Computation* 263, 378–391.

Jaffrin, M. Y. and A. H. Shapiro (1971). Peristaltic pumping. *Ann. Rev. Fluid Mech.* 3, 13-36.

Kothandapani, M. and S. Srinivas (2008). Peristaltic transport of a Jeffery fluid under the effect of magnetic field in an asymmetric channel.*Int. J. Non-linear Mech.* 43, 915-924.

Lakshminarayana, P., S. Sreenadh and G. Suchritha (2013). The influence of heat transfer on MHD peristaltic flow through a vertical asymmetric porous channel. *Elixir, Applied Mathematics* 54, 12413-12419.

Mishra, M. and A. Ramachandra Rao (2003). Peristaltic transport of a Newtonian fluid in an asymmetric channel. *ZAMP.* 54, 532–50.

Nadeem, S. and S. Akram (2010). Influence of inclined magnetic field on peristaltic flow of a Williamson fluid model in an inclined symmetric or asymmetric channel. *Mathematical and Computer Modelling* 52, 107-119.

Narahari, M. and S. Sreenadh (2010). Peristaltic transport of a Bingham fluid in contact with a Newtonian fluid. *Int. J. of Appl. Math. and Mech.* 6(11), 41–54.

Noreen Sher Akbar and S. Nadeem (2012). Peristaltic flow of a Phan-Thien-Tanner nanofluid in a diverging tube. *Heat Transfer - Asian Research* 41(1), 10–12.

Noreen Sher Akbar and S. Nadeem (2014). Exact solution of peristaltic flow of biviscosity fluid in an endoscope: A note. *Alexandria Engineering Journal.* 53, 449–454.

Ramesh, K. and M. Devakar (2015). The influence of heat transfer on peristaltic transport of MHD second grade fluid through porous medium in a vertical asymmetric channel. *Journal of Applied Fluid Mechanics* 8(3), 351-365.

Rashidi, M. M., D. D. Ganji and S. Dinarvand (2009). Explicit Analytical Solutions of the Generalized Burger and Burger–Fisher Equations by Homotopy Perturbation Method. *Numerical Methods for Partial Differential Equations* 25(2), 409-417.

Rathod, V. P. and D. Laxmi (2014). Effects of heat transfer on the peristaltic MHD flow of aBingham fluid through a porous medium in a channel. *Int. J. of Biomath. 7*(6), 1450060.

Ravikiran, G. and G. Radhakrishnamacharya (2015). Effect of homogeneous and heterogeneous chemical reactions on peristaltic transport of a Jeffrey fluid through a porous medium with slip condition. *Journal of Applied Fluid Mechanics.* 8(3) 521-528.

Shapiro, A. H., M. Y. Jaffrinand and S. L. Weinberg **(**1969). Peristaltic pumping with long wavelengths at low Reynolds number. *J. Fluid Mech.* 37, 799–825.

Shukla, J. B. and S. P. Gupta (1982). Peristaltic transport of a power law fluid with variable consistency. *J. Biomech. Engng.* 104, 182–186.

Singh, J. and R. Rathee (2011). Analysis of non-

Newtonian blood flow through stenosed vessel in porous medium under the effect of magnetic field.*Int. J. Phys. Sci.*6, 2497–2506.

Sreenadh, S., P. Lakshminarayana and G. Sucharitha (2011). Peristaltic flow of micropolar fluid in an asymmetric channel with permeable walls.*Int. J. of Appl. Math. and Mech.* 7(20), 18–37.

Srinivas, S. and M. Kothandapani (2009). The influence of heat and mass transfer on MHD peristaltic flow through a porous space with complaint wall. *Appl. Math. Comput.* 213, 197-208.

Srivastava, L. M. and V. P. Srivastava (1984). Peristaltic transport of blood: Casson model II.*J.Biomech.* 17, 821–829.

Sucharitha, G., S. Sreenadh and P. Lakshminarayana (2013). Non-linear peristaltic flow of pseudoplastic fluid in an asymmetric channel with porous medium. *Int.J. of Eng. Sci. and Tech.* 5(1), 106–113.

Tripathi, D. (2013). Study of transient peristaltic heat flow through a finite porous channel. *Mathematical and Computer Modelling* 57, 1270-1283.

Usha, S. and A. RamachandraRao (1997). Peristaltic transport of two-layered power-law fluids. *J. Biomech. Engng.* 119, 483-488.

Vajravelu, K., S. Sreenadh and P. Lakshminarayana (2011). The influence of heat transfer on peristaltic transport of a Jeffrey fluid in a vertical porous stratum. *Commun. Non-linear Sci. Numer. Simulat.* 16, 3107–3125.

Vajravelu, K., S. Sreenadh, G. Sucharitha and P. Lakshminarayana (2014). Peristaltic transport of aconducting Jeffrey fluid in an inclined asymmetric channel. *Int. J. of Biomath.*7(6), 1450064.

Vajravelu, K., S. Sreenadh, K. Rajinikanth and Ch. Lee (2012). Peristaltic transport of a Williamson fluid in asymmetric channels with permeable walls. *Nonlinear Analysis: Real world applications* 13(6), 2804–2822.

Vajravelu, K., S. Sreenadh, R. Hemadri and K. Murugeshan (2009). Peristaltic transport of a Cassonfluidin contact with a Newtonian fluid in a circular tube with permeable wall. *Int. J. Fluid Mech. Res.* 36, 244–254.

Vajravelu, K., S. Sreenadhand and V. Ramesh Babu (2005a). Peristaltic transport of a Hershel-Bulkley fluid in an inclined tube. *Int. J. Non-linear Mech.* 40, 83-90.

Vajravelu, K., S. Sreenadhand and V. Ramesh Babu (2005b). Peristaltic pumping of a Herschel–Bulkley fluid in a channel. *Appl. Math. Comput.* 169, 726–35.

APPENDIX

$$L_1=\frac{1}{\sigma^2}\frac{dp_0}{dx}+1,\quad L_2=\cosh\sigma h_1-\cosh\sigma h_2,$$

$$L_3=\sinh\sigma h_1-\sinh\sigma h_2\quad L_2^1=\cosh\sigma h_1+\cosh\sigma h_2,$$

$$L_3^1=\sinh\sigma h_1+\sinh\sigma h_2, L_4^1=\left(\frac{(h_1+h_2)\left(L_3^2-L_2^2\right)}{\left(L_3L_3^1-L_2L_2^1\right)}+(h_2-h_1)\right)$$

$$c_1=\frac{-c_2L_2}{L_3},\ c_2=\frac{L_1L_3(h_2+h_1)}{L_3L_3^1-L_2L_2^1}, L_4=\left(\frac{dp_0}{dx}\right)^3+3\sigma^2\left(\frac{dp_0}{dx}\right)^2,$$

$$L_5=\left(\frac{c_1}{2}\right)^3+3\left(\frac{c_1}{2}\right)\left(\frac{c_2}{2}\right)^2$$

$$L_6=\left(\frac{c_2}{2}\right)^3+3\left(\frac{c_1}{2}\right)^2\left(\frac{c_2}{2}\right),$$

$$L_7=\left(\frac{c_1}{2}\right)^3-\left(\frac{c_1}{2}\right)\left(\frac{c_2}{2}\right)^2,\quad L_8=\left(\frac{c_2}{2}\right)^3-\left(\frac{c_1}{2}\right)^2\left(\frac{c_2}{2}\right),$$

$$L_9=\left(\frac{c_1}{2}\right)^2-\left(\frac{c_2}{2}\right)^2\ L_{10}=\left(\frac{c_2}{2}+\frac{c_1}{2}\right)\frac{3L_1^2\sigma}{2},$$

$$L_{11}=\frac{3L_1^2\sigma}{2}\left(\frac{c_1}{2}-\frac{c_2}{2}\right), L_{12}=\left(\frac{c_2}{2}\right)^2+\left(\frac{c_1}{2}\right)^2$$

$$L_{13}=2\left(\frac{c_2}{2}\right)\left(\frac{c_1}{2}\right), L_{14}=\frac{L_{10}-L_{11}}{3}+L_1^3, L_{15}=\frac{L_{10}+L_{11}}{2\sigma},$$

$$L_{16}=3L_1L_9+\frac{6L_1^3}{\sigma^2}+\frac{L_{10}-L_{11}}{2\sigma^2}, L_{17}=3\sigma^4\left(\sigma^2+\frac{dp_0}{dx}\right),$$

$$L_{18}=\frac{6L_1^2}{\sigma^2}+2L_9, L_{19}=\frac{2L_{12}L_{17}}{3\sigma^2},\ L_{20}=\frac{L_{17}c_1c_2}{3\sigma^2},$$

$$L_{21}=\frac{8L_{12}L_{17}}{9\sigma^3},\ L_{22}=\frac{4c_1c_2L_{17}}{9\sigma^3}, L_{23}=\frac{L_{17}L_8}{\sigma^2},$$

$$L_{24}=\frac{L_1^2L_{17}}{\sigma^2}, L_{25}=\frac{(c_1+c_2)L_1L_{17}}{3\sigma}, L_{26}=\frac{(c_1+c_2)L_1L_{17}}{2\sigma^3}$$

$$L_{27}=\frac{c_2L_1L_{17}}{2\sigma^2},\ L_{28}=\frac{c_1L_1L_{17}}{2\sigma^2},$$

$$L_{29}=3\sigma^2\left(1+\frac{2}{\sigma^2}\frac{dp_0}{dx}+\left(\frac{dp_0}{dx}\right)^2\right),$$

$$L_{30}=\frac{L_{29}L_1}{2\sigma}, L_{31}=L_{14}-L_{24}-\frac{L_4}{\sigma^2},$$

$$L_{32}=L_{16}-L_{23}-\frac{6L_4}{\sigma^4}, L_{33}=L_{19}-2L_1L_{12},$$

$$L_{34}=\frac{8L_1L_{13}}{3\sigma}-L_{22},\ L_{35}=L_{20}-2L_1L_{13}$$

$$L_{36}=\frac{8L_1L_{12}}{3\sigma}-L_{21}$$

$$L_{37}=3\sigma L_7+15\frac{L_{30}c_2}{4\sigma^5}, L_{38}=\frac{15L_{30}c_1}{4\sigma^4},\ L_{39}=\frac{5L_{30}c_2}{2\sigma^3},$$

$$L_{40}=\frac{5L_{30}c_1}{4\sigma^2},\ L_{41}=\frac{L_{30}c_2}{2\sigma}, L_{42}=\frac{L_{30}c_1}{6},$$

$$L_{43}=\frac{15L_{30}c_1}{4\sigma^5}-L_{26}-3\sigma L_8, L_{44}=\frac{15L_{30}c_2}{4\sigma^4}, L_{45}=\frac{5L_{30}c_1}{2\sigma^3}-L_{25},$$

$$L_{46}=\frac{5L_{30}c_2}{4\sigma^2}, L_{47}=\frac{L_{30}c_1}{2\sigma}, L_{48}=\frac{L_{30}c_2}{6},$$

$$L_{49}=L_{31}h_1^3-L_{15}h_1^2+L_{32}h_1, L_{50}=\frac{L_5\cosh 3\sigma h_1+L\sinh 3\sigma h_1}{4}$$

$$L_{51}=\cosh 2\sigma h_1\left(L_{34}+L_{33}h_1\right), L_{52}=\sinh 2\sigma h_1\left(L_{36}+L_{35}h_1\right),$$

$$L_{53}=L_{27}+L_{37}h_1-L_{38}h_1^2+L_{39}h_1^3, L_{54}=-L_{40}h_1^4+L_{41}h_1^5-L_{42}h_1^6,$$

$$L_{55}=\sinh\sigma h_1\left(L_{53}+L_{54}\right), L_{56}=L_{28}+L_{43}h_1-L_{44}h_1^2+L_{45}h_1^3$$

$$L_{57}=-L_{46}h_1^4+L_{47}h_1^5-L_{48}h_1^6, L_{58}=\cosh\sigma h_1\left(L_{56}+L_{57}\right),$$

$$L_{59}=L_{49}+L_{50}+L_{51}+L_{52}+L_{55}+L_{58}, L_{60}=L_{32}h_2-L_{15}h_2^2+L_{31}h_2^3,$$

$$L_{61}=\frac{L_5\cosh 3\sigma h_2+L_6\sinh 3\sigma h_2}{4}, L_{62}=\cosh 2\sigma h_2\left(L_{34}+L_{33}h_2\right)$$

$$L_{63}=\sinh 2\sigma h_2\left(L_{36}+L_{35}h_2\right), L_{64}=L_{27}+L_{37}h_2-L_{38}h_2^2+L_{39}h_2^3,$$

$$L_{65}=-L_{40}h_2^4+L_{41}h_2^5-L_{42}h_2^6, L_{66}=\sinh\sigma h_2\left(L_{64}+L_{65}\right),$$

$$L_{67}=L_{28}L_{43}h_2-L_{44}h_2^2+L_{45}h_2^3, L_{68}=-L_{46}h_2^4+L_{47}h_2^5-L_{48}h_2^6$$

$$L_{69}=\cosh\sigma h_2\left(L_{67}+L_{68}\right), L_{70}=L_{60}+L_{61}+L_{62}+L_{63}+L_{66}+L_{69},$$

$$L_{71}=2\sigma L_{34}+L_{35}, L_{72}=L_{33}+2\sigma L_{36}, L_{73}=L_{37}+\sigma L_{28},$$

$$L_{74}=\sigma L_{43}-2L_{38}, L_{75}=3L_{39}-\sigma L_{44}, L_{76}=\sigma L_{45}-4L_{40}$$

$$L_{77}=5L_{41}-\sigma L_{46}, L_{78}=\sigma L_{47}-6L_{42}, L_{79}=\sigma L_{27}+L_{43},$$

$$L_{80}=\sigma L_{37}-2L_{44}, \; L_{81}=3L_{45}-\sigma L_{48}L_{77}$$

$$L_{82}=\sigma L_{39}-4L_{46},$$

$$L_{83}=5L_{47}-\sigma L_{40}, L_{84}=\sigma L_{41}-6L_{48},$$

$$L_{85}=3L_{31}h_1^2-2L_{15}h_1+L_{32}, L_{86}=3\sigma\left(\frac{L_5\sinh 3\sigma h_1+L_6\cosh 3\sigma h_1}{4}\right),$$

$$L_{87}=\sinh 2\sigma h_1\left(L_{71}+2\sigma L_{33}h_1\right), L_{88}=\cosh 2\sigma h_1\left(L_{72}+2\sigma L_{35}h_1\right)$$

$$L_{89}=L_{73}+L_{74}h_1+L_{75}h_1^2, L_{90}=L_{76}h_1^3+L_{77}h_1^4+L_{78}h_1^5,$$

$$L_{91}=\sinh\sigma h_1\left(L_{89}+L_{90}\right), L_{92}=L_{79}+L_{80}h_1+L_{81}h_1^2,$$

$$L_{93}=L_{82}h_1^3+L_{83}h_1^4+L_{84}h_1^5, \; L_{94}=\cosh\sigma h_1\left(L_{92}+L_{93}\right)$$

$$L_{95}=L_{85}+L_{86}+L_{87}+L_{88}+L_{91}+L_{94}, L_{96}=3L_{31}h_2^2-2L_{15}h_2+L_{32},$$

$$L_{97}=3\sigma\left(\frac{L_5\sinh 3\sigma h_2+L_6\cosh 3\sigma h_2}{4}\right), L_{98}=\sinh 2\sigma h_2\left(L_{71}+2\sigma L_{33}h_2\right),$$

$$L_{99}=\cosh 2\sigma h_2\left(L_{72}+2\sigma L_{35}h_2\right), L_{100}=L_{73}+L_{74}h_2+L_{75}h_2^2$$

$$L_{101}=L_{76}h_2^3+L_{77}h_2^4+L_{78}h_2^5, L_{102}=\sinh\sigma h_2\left(L_{100}+L_{101}\right),$$

$$L_{103}=L_{79}+L_{80}h_2+L_{81}h_2^2, L_{104}=L_{82}h_2^3+L_{83}h_2^4+L_{84}h_2^5,$$

$$L_{105}=\cosh\sigma h_2\left(L_{103}+L_{104}\right), L_{106}=L_{96}+L_{97}+L_{98}+L_{99}+L_{102}+L_{105}$$

$$L_{107}=L_2^1, L_{108}=L_3^1, L_{109}=L_{108}^2-L_{107}^2, L_{110}=\frac{-L_{108}\left(h_1+h_2\right)}{\sigma}+\frac{2}{\sigma^2}L_{107},$$

$$L_{111}=\sigma L_{108}\left(L_{59}+L_{70}\right)-L_{107}\left(L_{95}+L_{106}\right),$$

$$c_3=\frac{\frac{1}{\sigma^2}\frac{dp_0}{dx}(h_2+h_1)-\left(L_{59}+L_{70}\right)-c_4L_{108}}{L_{107}}, c_4=\frac{-\left(\frac{dp_0}{dx}L_{10}+L_{111}\right)}{L_{109}},$$

$$L_{112}=\cosh 3\sigma h_1-\cosh 3\sigma h_2, L_{113}=\sinh 3\sigma h_1-\sinh 3\sigma h_2,$$

$$L_{114}=\cosh 2\sigma h_1-\cosh 2\sigma h_2, L_{115}=h_1\cosh 2\sigma h_1-h_2\cosh 2\sigma h_2,$$

$$L_{116}=\sinh 2\sigma h_1-\sinh 2\sigma h_2, L_{117}=h_1\sinh 2\sigma h_1-h_2\sinh 2\sigma h_2$$

$$L_{118}=\frac{L_5L_{112}+L_6L_{113}}{4}, L_{119}=\frac{L_{114}\left(L_{71}+L_{72}-L_{35}\right)}{2\sigma},$$

$$L_{120}=\frac{\left(L_{73}+L_{79}\right)}{\sigma}+\frac{2\left(L_{75}+L_{81}\right)}{\sigma^2}+\frac{24\left(L_{77}+L_{83}\right)}{\sigma^5}$$

$$L_{121}=\frac{\left(L_{74}+L_{80}\right)}{\sigma^2}+\frac{6\left(L_{76}+L_{82}\right)}{\sigma^4}+\frac{120\left(L_{78}+L_{84}\right)}{\sigma^6},$$

$$L_{122}=\frac{2\left(L_{75}+L_{81}\right)}{\sigma^2}+\frac{24\left(L_{77}+L_{83}\right)}{\sigma^4}$$

$$L_{123}=\frac{\left(L_{74}+L_{80}\right)}{\sigma}+\frac{6\left(L_{76}+L_{82}\right)}{\sigma^3}+\frac{120\left(L_{78}+L_{84}\right)}{\sigma^5},$$

$$L_{124}=\frac{\left(L_{75}+L_{87}\right)}{\sigma}+\frac{12\left(L_{77}+L_{83}\right)}{\sigma^3}$$

$$L_{125}=\frac{3\left(L_{76}+L_{82}\right)}{\sigma^2}+\frac{60\left(L_{78}+L_{84}\right)}{\sigma^4},$$

$$L_{126}=L_{31}+L_3\left(\frac{\left(L_{76}+L_{82}\right)}{\sigma}+\frac{20L_{84}}{\sigma^3}\right)-4L_2\frac{\left(L_{77}+L_{83}\right)}{\sigma^2}$$

$$L_{127}=\frac{L_3\left(L_{77}+L_{83}\right)}{\sigma}-\frac{5L_2\left(L_{78}+L_{84}\right)}{\sigma^2},$$

$$L_{128}=L_{118}+L_{119}+L_3L_{120}-L_2L_{121}$$

$$L_{129}=\left(h_1-h_2\right)\left(L_{32}-L_2L_{122}+L_3L_{123}\right)+\left(h_1^2-h_2^2\right)\left(L_3L_{124}-L_2L_{125}-L_{15}\right)$$

$$L_{130}=\left(h_1^3-h_2^3\right)L_{126}+\left(h_1^4-h_2^4\right)L_{127}+\frac{\left(h_1^5-h_2^5\right)}{\sigma}L_3$$

$$L_{131}=\frac{\left(h_1+h_2\right)L_2L_{109}+\sigma^2L_{110}L_{108}-\sigma^2L_3L_{107}-\left(h_1-h_2\right)L_{107}L_{109}}{\sigma^2L_{107}L_{109}}$$

$$L_{132}=L_{128}+L_{129}+L_{130}+\left(\frac{L_{117}\left(L_3L_{107}-L_{108}\right)-L_{109}L_2\left(L_{59}+L_{70}\right)}{L_{107}L_{109}}\right)$$